Telemanipulation of Snake-Like Robots for Minimally Invasive Surgery of the Upper Airway

Abstract. This research focuses on developing and testing the high-level control of a novel 8 DoF hybrid robot using a DaVinci master manipulator. The teleoperation control is formulated as two weighted, multi objective constrained least square (LS) optimization problems - one for the master controller and the other for the slave controller. This allows us to incorporate various virtual fixtures in our control algorithm as constraints of the LS problem based on the robot environment. Experimental validation to assure position tracking and sufficient dexterity to perform suturing in confined spaces such as throat are presented.

Minimally invasive surgery (MIS) of the chest and abdomen provides multiple ports to access the anatomy and allows large motions at the proximal joints of telesurgical slave robots. Compared to MIS of the chest and abdomen, it is vital to minimize the motions of the proximal joints in single entry port MIS due to strict space limitations. In addition, the slave robots must have high distal dexterity and a large number of DoF. This paper presents a general high-level control method for telemanipulation using a linear least squares optimization framework. This framework allows easy incorporation of virtual fixtures in high-DOF telesurgical systems for single entry port MIS. The validation of our framework is performed on a novel system for MIS of the throat [1] using a DaVinci Master manipulator in our laboratory.

MIS of the throat is characterized by a single entry port (patients mouth) through which surgical tools operate. Current manual tools are hard to manipulate precisely, and lacks sufficient dexterity to permit common surgical tasks such as suturing. This clinical problem motivated the development of a novel system for MIS of the upper airway. Our proposed solution is a telesurgical robot with a hybrid slave manipulator that has a snake-like unit (SLU) for its distal end, which provides high tool-tip dexterity. In previous works [2–5] novel telesurgical slave robots implementing snake-like units for distal dexterity enhancement were presented, but few address the issue of human interfaces to these complex mechanisms. Csencsits et al. [6] evaluated interfaces for snake-like devices using joysticks. Our method allows the addition of virtual fixtures to enable intuitive control of snake-like devices by a human user. Moreover, virtual fixtures can be used to augment MIS tasks that require better-than-human levels of precision.

Virtual fixtures (VF), which have been discussed previously in the literature for cooperative robots [7–9], are algorithms which provide anisotropic behavior to surgeons motion command besides filtering out tremor to provide safety and precision. Virtual fixtures have been implemented on impedance-type teleoperators under various forms in [10–12]. It has been shown that implementing forbidden-region virtual fixtures using impedance control techniques can lead to instability [13]. Moreover, these works are based either on a specific robot type

(admittance or impedance) or on a specific task. We present a method that covers implementation of both guidance and forbidden regions and is suitable for both types of robots. In doing this we extend the work of Funda et al. [14] and Li and Taylor [15] to teleoperated systems with impedance-type master robots. This will enable us to implement stable virtual fixtures on these types of robots.

1 Methods

1.1 Control Algorithm Overview

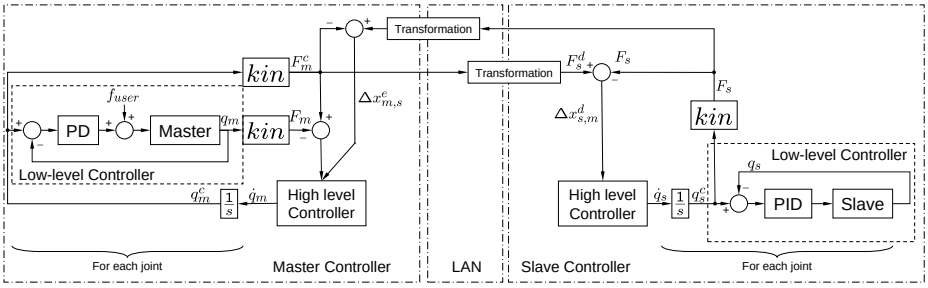

Fig. 1. Block diagram of current implementation of master-slave controller

In this section we outline a new method to address telemanipulation of an admittance-type snake-like robot using an impedance-type robot. To achieve this we mimic an admittance-type behavior on the master manipulator. The overall structure of the control algorithm is shown in Figure 1. There are separate controllers for the master and the slave connected through a communication network. The overall method works as follows

1. Individual joints of the manipulator are servoed with low-level controllers (PD or PID) to set points. A desired Cartesian velocity is calculated for each manipulator.
2. A constrained least squares problem is solved for the joint velocities by the high-level controller. The least square problem has an objective function describing desired outcome. It may also include constraints that consider any motion constraints due to VF, joint limits, and velocity limits. This problem has the general form of

$$\begin{aligned} &\arg\min_{\Delta \boldsymbol{q}_r/\Delta t} \|(A_r(\boldsymbol{q}_r, \dot{\boldsymbol{q}}_r) \cdot \Delta \boldsymbol{x}_r/\Delta t - \Delta \boldsymbol{x}_r^d/\Delta t)\|, \\ s.t. \quad &H_r(\boldsymbol{q}_r, \dot{\boldsymbol{q}}_r) \cdot \Delta \boldsymbol{x}_r/\Delta t \geq \boldsymbol{h}_r, \quad \text{and} \quad \Delta \boldsymbol{x}_r/\Delta t = J_r \Delta \boldsymbol{q}_r/\Delta t \end{aligned} \tag{1}$$

where $r \in \{m, s\}$ for master or slave. $\Delta \boldsymbol{q}_r$ is the desired incremental motion of the joint variables. The desired incremental motion in Cartesian space, $\Delta \boldsymbol{x}_r^d = g(\boldsymbol{f}, \boldsymbol{q}_r)$ is a function of user's input, $\boldsymbol{f}$, and joint variables, $\boldsymbol{q}_r$. Matrix J_r is the Jacobian of the manipulator. Δt is the small time interval of high-level control loop. Matrices H_r and A_r along with vector $\boldsymbol{h_r}$ define the behavior of the robot to a given input.

3. Numerically integrate the joint velocities to arrive at a new set of joint positions. We assume that for each iteration loop, the incremental motions are sufficiently small and $\Delta \boldsymbol{x}_r/\Delta t = J_r \Delta \boldsymbol{q}_r/\Delta t$ represents a good approximation to the relationship between $\Delta \boldsymbol{x}_r/\Delta t$ and $\Delta \boldsymbol{q}_r/\Delta t$.

1.2 Implementation on Master Manipulator

In this section, we discuss the desired behavior of the master manipulator to an user input and formulate a specific constrained least square problem based on the general form presented in (1). We model the manipulator as a kinematic device having a position $\boldsymbol{p}_m \in \Re^3$ and orientation given by a rotation matrix $R_m \in \Re^{3\times 3}$. The frame $F_m = \left(R_m, \boldsymbol{p}_m\right)$ is computed using the actual encoder joint positions and the frame $F_m^c = \left(R_m^c, \boldsymbol{p}_m^c\right)$ is computed using the commanded joint positions (reference set points for servo controller) using forward kinematics.

Desired Cartesian Velocity In the admittance-type devices a force sensor measures the user input, $\boldsymbol{f}$. The desired Cartesian velocity is computed by multiplying the user input by the user supplied admittance gain matrix K_a. It has been shown in [16] that for 3 DoF impedance-type robots, under quasi-static condition, the applied user force can be measured approximately by the position error. We extend it to the 6 DoF case by defining the position and orientation errors as $\boldsymbol{p}_m^e = \boldsymbol{p}_m^c - \boldsymbol{p}_m$ and $R_m^e = R_m^c \cdot R_m^{-1}$, respectively. Further we make use of the small angle approximation to Rodriguez formula for the orientation error,

$$R_m^e = I + (\sin\theta_m)\hat{\boldsymbol{\omega}}_m + (1-\cos\theta_m)(\hat{\boldsymbol{\omega}}_m)^2 \approx I + \theta_m \hat{\boldsymbol{\omega}}_m;\ \left\|\boldsymbol{\omega}_m\right\|_2 = 1 \qquad (2)$$

where $\hat{\boldsymbol{\omega}}_m$ is a skew symmetric matrix corresponding to vector $\boldsymbol{\omega}_m$. Scalar θ_m is magnitude of rotation angle about $\boldsymbol{\omega}_m$. We can replace the force sensor measurement in the admittance control law by a wrench that is a six vector obtained by concatenating $\boldsymbol{p}_m^e$ and $\theta_m \boldsymbol{\omega}_m$, that is, $\Delta \boldsymbol{x}_m^d/\Delta t = K_a \left[\boldsymbol{p}_m^e\ ; \theta_m \boldsymbol{\omega}_m\right]$. A small dead-band is used on this error to avoid motion that might arise due to small errors in the servo control.

Objective function We identify three objective criteria for the tip frame that are required to achieve desired motion of the tip. First, we require that an incremental motion be as close as possible to the desired Cartesian velocity. We express this as: $\min_{\Delta \boldsymbol{q}_m/\Delta t} \left\|\Delta x_m/\Delta t - \Delta \boldsymbol{x}_m^d/\Delta t\right\|$.

A teleoperator virtually connects the master and slave tips. The slave follows the master positions, but the master must also provide resistance to the user based on the position of the slave and/or the force at the slave tip. We model this virtual coupling as a spring, which results in: $\min_{\Delta \boldsymbol{q}_m/\Delta t} \left\|\Delta x_m/\Delta t - \Delta \boldsymbol{x}_{m,s}^e/\Delta t\right\|$, where $\Delta \boldsymbol{x}_{m,s}^e$ is a function of both the master and slave positions. We defer the discussion on computation of $\Delta \boldsymbol{x}_{m,s}^e$ until section 1.3.

Finally we would like to minimize the extraneous motion of the joints, and avoid large incremental joint motions that could occur near singularities, that is, $\min_{\Delta \boldsymbol{q}_m/\Delta t} \left\|\Delta \boldsymbol{q}_m/\Delta t\right\|$.

We can project the Cartesian tip motion to the joint motion via the Jacobian relationship, and use three diagonal matrix of weighting factors $W_{m,t}$, $W_{m,s}$ and $W_{m,j}$ associated with each of the objectives, to obtain the final objective function to be minimized. The final objective function is

$$\min_{\Delta \boldsymbol{q}_m} \left\| \begin{bmatrix} W_{m,t} & \mathbf{0} & \mathbf{0} \\ \mathbf{0} & W_{m,s} & \mathbf{0} \\ \mathbf{0} & \mathbf{0} & W_{m,j} \end{bmatrix} \begin{bmatrix} J_m \\ J_m \\ I \end{bmatrix} \Delta \boldsymbol{q}_m - \begin{bmatrix} \Delta \boldsymbol{x}_m^d \\ \Delta \boldsymbol{x}_{m,s}^e \\ \mathbf{0} \end{bmatrix} \right\| \tag{3}$$

The diagonal elements of $W_{m,t}$ specify the relative importance of each component of $\Delta \boldsymbol{x}_m$. The ratio of diagonal elements of $W_{m,s}$ to elements of $W_{m,t}$ specify the "stiffness" of the virtual spring connecting the master, and the slave tips. A factor close to zero implies a loose connection or no connection. The ratios between the elements of $W_{m,j}$ themselves can be used to favor motion of some joints over others. We must ensure proper scaling of weights corresponding to different components. Otherwise, the result of the optimization $\Delta \boldsymbol{q}_m$ will cause incorrect control behavior.

Optimization constraints By defining instantaneous motion relationships between different task frames $\{i\}$ and the incremental joint motions we can implement VF for those task frames. The relationship has the form

$$H_{m,i} J_{m,i}(\boldsymbol{q}_m) \Delta \boldsymbol{q}_m \geq \boldsymbol{h}_{m,i} \tag{4}$$

where $J_{m,i}(\boldsymbol{q}_m)$ is the Jacobian relating Cartesian task frame vector, $\Delta \boldsymbol{x}_{m,i}$ to the incremental joint motion. In [17] we had proposed a library of five primitives that could be used to create VF for different tasks by appropriately selecting matrix $H_{m,i}$ and vector $\boldsymbol{h}_{m,i}$. Currently we have implemented two sets of constraints for joint limits and joint velocities. The two set of limit constraints can be combined to give the following set of equations

$$H_{m,j} \Delta \boldsymbol{q}_m \geq \boldsymbol{h}_{m,j}; \quad \text{where} \quad H_{m,j} = \begin{bmatrix} I \\ -I \\ I \\ -I \end{bmatrix} \quad \text{and} \quad \boldsymbol{h}_{m,j} = \begin{bmatrix} \boldsymbol{q}_{m,L} - \boldsymbol{q}_m \\ \boldsymbol{q}_m - \boldsymbol{q}_{m,U} \\ \dot{\boldsymbol{q}}_{m,U} \cdot \Delta t \\ \dot{\boldsymbol{q}}_{m,U} \cdot \Delta t \end{bmatrix} \tag{5}$$

where $\boldsymbol{q}_{m,L}$ and $\boldsymbol{q}_{m,U}$ are lower and upper bounds of joint ranges and $\dot{\boldsymbol{q}}_{m,U}$ is the upper bound of the joint velocities.

1.3 Implementation on Slave Manipulator

In this section we discuss objective and constraints for the slave device optimization problem.

Desired Cartesian Motion We define two frames called the neutral frames that are specific tip frames of master and slave, chosen by the user. They are chosen such that the user perceives through the Head Mounted Display (HMD) that the slave gripper is aligned with her hand orientation. We denote the tip frame of the master with respect to a neutral frame as ${}^{m,0}F_m = ({}^{m,0}R_m, {}^{m,0}\boldsymbol{p}_m)$

and neutral frame of the slave with respect to its base frame as ${}^{w,s}F_{s,0} = ({}^{w,s}R_{s,0}, {}^{w,s}\boldsymbol{p}_{s,0})$. For the user to always perceive the slave gripper is aligned with her hand, we require that the slave tip motion with respect to its neutral position be same as master tip motion with respect to its neutral. That is, slave tip frame with respect to its base frame is ${}^{w,s}F_s^d = (R_s^d, \boldsymbol{p}_s^d) = {}^{w,s}F_{s,0} \cdot {}^{m,0}F_m$.

A six vector $\Delta\boldsymbol{x}_{s,m}^d$ can be computed by taking the difference between the desired frame and the current slave tip frame. The matrix $R_s^e = R_s^d \cdot R_s^{-1}$ can be converted to a three vector by using the Rodriguez formula in (2) or its small angle approximation if applicable. Thus, $\Delta\boldsymbol{x}_{s,m}^d = \left[\boldsymbol{p}_s^d - \boldsymbol{p}_s; \bigvee(R_s^e)\right]$. The computation of $\Delta\boldsymbol{x}_{m,s}^e$ required in (3) can be accomplished by exchanging the roles of master and slave in the above discussion.

Objective function The objective function for the slave has two criteria; one for following the desired motion and the other to restrict extraneous motion of the joints. The final equation is

$$\min_{\Delta\boldsymbol{q}_s} \left\| \begin{bmatrix} W_{s,t} & \mathbf{0} \\ \mathbf{0} & W_{m,j} \end{bmatrix} \begin{bmatrix} J_s \\ I \end{bmatrix} \Delta\boldsymbol{q}_s - \begin{bmatrix} \Delta\boldsymbol{x}_s^d \\ \mathbf{0} \end{bmatrix} \right\| \tag{6}$$

Optimization constraints Besides the joint limit and joint velocity constraints we also have additional constraints on the motion of slave manipulator. Our slave manipulator has been designed specifically for MIS of the throat. In throat surgery the entry port is predetermined (the patient's mouth) and multiple tools have to pivot through a long and narrow laryngoscope about a point inside the laryngoscope. This creates a need for a iso-center ("Remote Center of Motion" (RCM)) at that point either through software (VRCM) or through mechanism design (e.g. [18]). The VRCM point is implemented using a form of (4). In this section we discuss the matrix $H_{s,c}$ and vector $\boldsymbol{h_{s,c}}$ which replaces the matrix $H_{m,i}$ and the vector $\boldsymbol{h_{m,i}}$ for the specific case of VRCM. The VRCM point is represented by $\boldsymbol{p}_{s,vrcm}$ in the base coordinate frame of the slave. Frame $F_{s,p} = (R_{s,p}, \boldsymbol{p}_{s,p})$ is associated with a convenient point on a tool shaft, such that the Z-axis of this frame, $\hat{\boldsymbol{r}_z}$ is aligned with the tool shaft.

Let $\boldsymbol{p}_{s,c}$ be the closest point to $\boldsymbol{p}_{s,vrcm}$ on the line from point $\boldsymbol{p_{s,p}}$ with direction $\hat{\boldsymbol{r}}_z$. We define a frame $\{c\}$ with origin $\boldsymbol{p}_{s,c}$ and same orientation as $F_{s,p}$. To satisfy the VRCM constraint we require the length of vector $\boldsymbol{d} = (\boldsymbol{p}_{s,c} - \boldsymbol{p}_{s,vrcm})$ after the incremental joint motion be less than a small value ϵ. If Jacobian $J_{s,c}$ relates the Cartesian velocities of frame $\{c\}$ with joint velocities of the slave, then after the incremental joint motion $\boldsymbol{d}$ becomes $\boldsymbol{e} = \boldsymbol{p}_{s,c} + J_{s,c}(1:3,:) \cdot \Delta\boldsymbol{q}_s - \boldsymbol{p}_{s,vrcm}$ and $\left\|\boldsymbol{e}\right\| \leq \epsilon$. The magnitude of ϵ indicates the allowed tolerance in the VRCM point. For computation efficiency we solve a least squares problem with linear constraints. We can linearize this distance constraint by considering projections of $\boldsymbol{e}$ on a finite number of lines through $\boldsymbol{p}_{s,c}$. If R_{vrcm} is any rotation matrix with $\hat{\boldsymbol{r}}_z$ as the third column, then

$$\left[R_{vrcm}\left[c_{\gamma i};\, s_{\gamma i};\, 0\right]\right]^t \boldsymbol{e} \leq \epsilon; \quad c_{\gamma i} = \cos\frac{2\pi i}{k};\; s_{\gamma i} = \sin\frac{2\pi i}{k};\; i = 1, \cdots, k \tag{7}$$

Let $H_{s,j}$ and $\boldsymbol{h_{s,j}}$ be similar to $H_{m,j}$ and $\boldsymbol{h_{m,j}}$ in (5), with the values of $\boldsymbol{h_{m,j}}$ replaced appropriately for the slave manipulator. By using the Jacobian $J_{s,c}$ to project to joint space and a rearrangement of (7) the complete set of constraints for the slave can be written as

$$\begin{bmatrix} H_{s,c} & \mathbf{0} \\ \mathbf{0} & H_{s,j} \end{bmatrix} \cdot \begin{bmatrix} J_{s,c} \\ I \end{bmatrix} \cdot \Delta \boldsymbol{q}_s \geq \begin{bmatrix} \boldsymbol{h_{s,c}} \\ \boldsymbol{h_{s,j}} \end{bmatrix};\ H_{s,t} = \begin{bmatrix} \cdots \\ \left[-R_{vrcm}\left[c_{\gamma i};\ s_{\gamma i};\ 0\right];\ \mathbf{0}\right]^t \\ \cdots \end{bmatrix} \tag{8}$$

where $H_{s,c} \in \Re^{k\times 6}$ and $\boldsymbol{h_{s,c}} = \left[\cdots\ ;\ -\epsilon;\ \cdots\right] + H_{s,c} \cdot \left[\boldsymbol{d};\ \mathbf{0}\right] \in \Re^k$.

2 Experimental Setup

The experimental setup consists of a DaVinci master which is a 7 DoF haptic device, a custom 8 DoF hybrid slave manipulator and a stereo vision system. The master is a commercially available system with its controller replaced by custom hardware and software, thus allowing us greater flexibility in control. The servo loops have a sampling rate of $1kHz$. The devices communicate over TCP network with a sampling rate of $100Hz$, which is the same as the sampling rate for the local high-level control loop. The gains of PD servo controller are chosen such that the settling time is less than the sampling rate of master high-level loop. This ensures that quasi-static approximation required in section 1.2 is met. The vision system consists of a stereo laparoscopic camera mounted at the end of a passive arm. The video streams are displayed on a HMD worn by the user.

The hybrid slave manipulator is unique and its design was motivated by MIS of the upper airway including the throat and larynx. The final embodiment of our proposed slave robot consists of two snake-like units (SLU) that are actuated through long tubes using Nitinol wires. A two-jaw detachable gripper is attached to the end of the SLU. The actuators for the SLU are mounted on a 4 DoF $XY\Theta Z$ manipulator. The ΘZ is connected to XY using a 2 DoF passive joints.

While the final slave is being fabricated, we have attached one SLU to an available 6 DoF manipulator to conduct preliminary experiments using our teleoperator control algorithm. In the current implementation the 6 DoF manipulator has three XYZ stages that are serially attached to a RCM mechanism. The axis of rotation of the third rotary joint passes through this remote point. The long shaft of the SLU actuators is aligned with the third rotary axis. For this work we have chosen the frame $F_{s,p}$ defined in section 1.3 to be origin of the frame assigned to the fifth DoF. Though the current implementation has a RCM by mechanism design, it was not at an appropriate position with respect tool tip. Thus we use the VRCM constraint to provide a suitable RCM point.

3 Results and Discussion

The robots described in section 2 had been tested using our high-level control algorithm. The tracking responses are given in Figures 2(a) and 2(b). For the

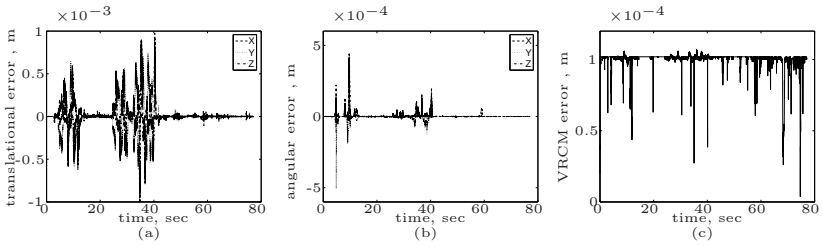

Fig. 2. (a) Master-Slave tracking response, linear components (b) Master-Slave tracking response, angular components (c) Error in the VRCM point

error in slave orientations we compute the angles between the desired and actual X, Y and Z axes. Figure 2(c) shows the norm of the error in VRCM point, $(\boldsymbol{p}_{s,c} - \boldsymbol{p}_{s,vrcm})$, as defined in section 1.3. For the experiments we used $\epsilon = 0.1mm$.

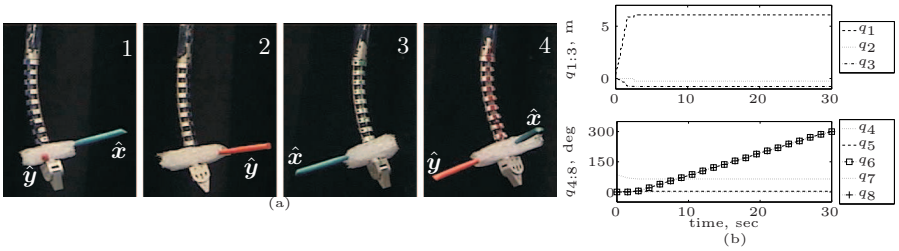

Fig. 3. (a) Series of pictures showing roll motion of gripper. $\hat{\boldsymbol{x}}$ and $\hat{\boldsymbol{y}}$ represent the X and Y axes of gripper frame. (b) Corresponding motion of slave joints. $q_{1:3}$ are XYZ, $q_{4:6}$ are three rotary joints and $q_{7:8}$ are the parameterization of the SLU configuration.

Suturing using a curved needle in confined workspace requires large dexterity at the distal end and sufficient roll about the gripper axis. Figure 3(a) shows a series of pictures taken during one of these roll motions. As seen in Figure 3(b), we require no movement of the proximal end of the slave manipulator to perform the roll motion. This has potential benefits in laryngeal surgery as multiple instruments need to be used through a narrow opening of the laryngoscope. Thus, little or no motion of joints at the proximal end minimizes tool collision and gives the surgeon sufficient access to the surgical site. We are currently evaluating this setup with a simple suturing phantom for *ex vivo* suturing.

4 Conclusions and Future Work

We have presented the high-level control of a telesurgical system designed considering the special requirements of MIS of throat. The high level control is based on linearized constraints, multi-objective least square optimization problem that is easily extendable to include additional constraints such as collision avoidance, anatomic-based constraints [15] and joint limits. On the slave side, the specific requirement of a remote center of motion was formulated as constraints compatible with the optimization framework.

We have performed successful validation of our control using an experimental 8-DoF robot, composed of a 6 DoF robot and Snake-Like Unit (SLU) used for

distal dexterity. The dexterity of the SLU was effectively used to provide roll movement of the gripper, without any motions of the proximal joints. This is a crucial requirement for suturing in confined spaces, such as the throat.

To conduct user performance based evaluation of most common surgical tasks a second arm (SLU) is necessary. Currently this is being fabricated along with a custom 4 DoF device to manipulate the arm. The current results serve as a validation of our control to be used in the final version of a novel telerobotic system for MIS of the throat. The current work also provides a basis for implementing virtual fixtures in impedance-type robots for complex tasks such as suturing.

References

1. (Anonymous)
2. Peirs, J., et al.: Design of an advanced tool guiding system for robotic surgery. In: ICRA. (2003) 2651–2656
3. Takahashi, H., et al.: Development of high dexterity minimally invasive surgical system with augmented force feedback capability, BioRob (2006)
4. Ikuta, K., et al.: Development of remote microsurgery robot and new surgical procedure for deep and narrow space. In: ICRA. (2003) 1103 – 1108
5. Charles, S., et al.: Dexterity-enhanced telerobotic microsurgery. In: ICAR. (1997) 5–10
6. Csencsits, M., et al.: User interfaces for continuum robot arms. In: IROS. (2005) 3123 – 3130
7. Davies, B.L., et al.: Active compliance in robotic surgerythe use of force control as a dynamic constraint. Proc Inst Mech Eng [H]. **211**(4) (1997) 285–292
8. Itoh, T., Kosuge, K., Fukuda, T.: Human-machine cooperative telemanipu- lation with motion and force scaling using task-oriented virtual tool dynamics. IEEE Trans. Robotics and Automation **16**(5) (2000) 505–516
9. Marayong, P., et al.: Spatial motion constraints: Theory and demonstrations for robot guidance using virtual fixtures. In: ICRA. (2003) 1954–1959
10. Rosenberg, L.B.: Virtual fixtures: Perceptual tools for telerobotic manipulation. In: IEEE Virtual Reality Annual International Symposium. (1993) 76–82
11. Park, S., et al.: Virtual fixtures for robotic cardiac surgery. In: MICCAI. (2001) 1419 – 1420
12. Turro, N., Khatib, O.: Haptically augmented teleoperation, Intl. Symposium on Experimental Robotics (2000) 1–10
13. Abbott, J.J., Okamura, A.M.: Analysis of virtual fixture contact stability for telemanipulation. In: IROS. (2003) 2699 – 2706
14. Funda, J., et al.: Constrained cartesian motion control for teleoperated surgical robots. IEEE Trans. Robot. Automat. **12**(3) (1996) 453–465
15. Li, M., Taylor, R.H.: Spatial motion constraints in medical robot using virtual fixtures generated by anatomy. In: ICRA. (2004) 1270–1275
16. Abbott, J.J., et al.: Steady-hand teleoperation with virtual fixtures. In: 12th IEEE Workshop on Robot and Human Interactive Communication. (2003) 145–151
17. (Anonymous)
18. Kumar, R., et al.: An augmentation system for fine manipulation. In: MICCAI. (2000) 956 – 965